THE ASTROPHYSICAL JOURNAL, 352:561–573, 1990 April 1


# NEAR-INFRARED EMISSION-LINE SPECTRA OF THE ORION NEBULA, NGC 4151, AND OTHER SEYFERT GALAXIES[1]

DONALD E. OSTERBROCK, RICHARD A. SHAW, AND SYLVAIN VEILLEUX
University of California Observatories/Lick Observatory and Board of Studies in Astronomy and Astrophysics, University of California, Santa Cruz
*Received 1989 July 17; accepted 1989 September 25*

## ABSTRACT

Near-infrared CCD spectra, covering the wavelength interval of approximately λλ7000–11000 at moderate resolution (FWHM ≈ 6 Å), were obtained of NGC 1976 and NGC 4151 in three overlapping segments. The wavelengths and relative line fluxes were measured, and most of the lines were identified. The strongest three lines in both objects are, in order, [S III] λ9531, He I λ10830, and [S III] λ9069. The Orion Nebula spectrum is very helpful for identifying lines in NGC 4151 and for comparison with it. Among the ions identified in NGC 1976, many of them previously known, are [Fe II], [Ni II], [Ni III], [Cl II], and [C I]. Likewise, in NGC 4151, [C I], [Fe II], [Fe XI], [Cl II], [Ni II], [Ar III], [Ar V], and [S II] are all present, and probably [S VIII] as well, in addition to H I, He I, and He II.

Lower resolution (FWHM ≈ 12 Å) spectra covering the range λλ7000–10000 of 14 additional Seyfert galaxies were also obtained and measured. The strongest line in all but two of them is [S III] λ9531. Nearly all these galaxies show the strongest [Ni II] line, λ7378. Comparison of line strengths among these various Seyfert galaxies allow the ionization behavior to be traced. One unidentified line, λ7865, that is present in the spectra of NGC 4151, III Zw 77, and three other galaxies, is probably a high-ionization forbidden line. Two other unidentified emission lines apparently observed in two or more Seyfert galaxies are λ9138 and λ9191.

The best additional diagnostic information the near-infrared spectral region provides, the [S III] (λ9069 + λ9531)/λ6312 ratio, is not as useful as the analogous [O III] ratio, due to the blending of λ6312 and the greater wavelength interval of the [S III] ratio.

*Subject headings:* galaxies: individual (NGC 4151) — galaxies: Seyfert — infrared: spectra — line identifications — nebulae: Orion Nebula

## I. INTRODUCTION

Much has been learned from the optical emission-line spectra of Seyfert galaxies and other active galactic nuclei, though much more remains to be learned. Ultraviolet and infrared spectra have, in recent years, added more information. With the advent of CCD detectors, it has become possible to extend the optical measurements into the near-infrared spectral region, from the previous IDS working limit of about 8000 Å out to about 11000 Å, although the sensitivity falls off rapidly in the last 1000 Å or so. Clearly, still more astrophysical information should be available in this near-infrared region.

Very important pioneering work in this spectral region was done by Andrillat and Collin-Souffrin (1975) and by Boksenberg *et al.* (1975). More recently, the Ca II λλ8498, 8542, 8662 emission lines have been measured in many Seyfert galaxies by Persson and McGregor (1985) and Persson (1988). Also, the whole near-infrared spectral region has been surveyed in many objects, particularly southern Seyfert galaxies, by Morris and Ward (1988). We have, in the past three years, begun observing Seyfert galaxies in this region also, and we present our results to date in this paper.

## II. OBSERVATIONS

All the spectra presented here were obtained with the UV-Schmidt spectrograph and a thinned TI 800 × 800 three-phase CCD detector (Lauer *et al.* 1984) attached to the Cassegrain focus of the Shane 3 m telescope of Lick Observatory. All of the objects were observed using a 3″ × 72″ slit. Spectra of all the Seyfert galaxies were obtained at low dispersion using a 300 lines $mm^{-1}$ grating, which gave a resolution (FWHM) of ∼12 Å and covered the approximate spectral range 6950–10050 Å. Higher dispersion spectra of the Orion nebula, NGC 1976, and of the bright Seyfert galaxy NGC 4151 were also obtained using a 600 lines $mm^{-1}$ grating with a resolution of ∼6 Å. Three different grating rotations were used to cover the spectral range λλ6950–11000 (with some overlap): exposures covering λλ6950–8550 were obtained using a grating blazed at 5000 Å, while exposures covering λλ8150–9750 and λλ9400–11000 were obtained using a different grating blazed at 7500 Å. A journal of the observations is presented in Table 1. Listed in order are the name of the object, the UT date of the observation, the central wavelength, the dispersion used ("N" and "H" stand for the observations obtained with the 300 line $mm^{-1}$ grating and the 600 lines $mm^{-1}$ grating, respectively), and the exposure time.

### *a) Basic Data Reduction*

The spectra were extracted from bias and flat field–corrected images. There is strong fringing in the near-IR, approaching 20% peak-to-peak. Since the intensity of the flat field lamp and the grating blaze function change very slowly and smoothly with wavelength, the lamp also revealed a steep drop in the CCD sensitivity longward of about 8000 Å; the sensitivity drops sharply once again at about 1 μm. The spectrum of each object was not extracted from the CCD image by simply summing the counts of the columns containing the spectrum, both because the UV-Schmidt spectrograph produces slightly

[1] *UCO/Lick Observatory Bulletin* No. 1147.

TABLE 1

JOURNAL OF OBSERVATIONS

| Object | UT Date | $\lambda_c$ (Å) | Grating | Exposure (minutes) |
|---|---|---|---|---|
| NGC 1976 .......... | 1988 Mar 21 | 7750 | H | 10 |
| | | 7750 | H | 60 |
| | 1988 Mar 22 | 8960 | H | 5 |
| | | 8960 | H | 60 |
| | | 10200 | H | 5 |
| | | 10200 | H | 60 |
| NGC 1320 .......... | 1987 Nov 15 | 8610 | N | 60 |
| NGC 3227 .......... | 1987 Nov 15 | 8610 | N | 60 |
| NGC 3516 .......... | 1988 Mar 21 | 8520 | N | 60 |
| NGC 4051 .......... | 1988 Mar 21 | 8520 | N | 60 |
| NGC 4151 .......... | 1988 Mar 21 | 8520 | N | 30 |
| | 1988 Mar 22 | 7750 | H | 10 |
| | | 7750 | H | 60 |
| | | 8960 | H | 10 |
| | | 8960 | H | 60 |
| | | 10200 | H | 60 |
| NGC 6814 .......... | 1986 Sep 3 | 8550 | N | 30 |
| NGC 7469 .......... | 1986 Sep 3 | 8550 | N | 60 |
| Mrk 1 ............... | 1986 Sep 4 | 8550 | N | 60 |
| Mrk 3 ............... | 1987 Nov 15 | 8610 | N | 60 |
| Mrk 915 ............ | 1986 Sep 4 | 8550 | N | 60 |
| Mrk 993 ............ | 1986 Sep 3 | 8550 | N | 80 |
| Mrk 1126 .......... | 1986 Sep 4 | 8550 | N | 60 |
| I Zw 1 ............... | 1987 Nov 15 | 8610 | N | 60 |
| II Zw 136 .......... | 1986 Sep 3 | 8550 | N | 60 |
| III Zw 77 ............ | 1986 Sep 4 | 8550 | N | 90 |
| VII Zw 31 .......... | 1988 Mar 21 | 8520 | N | 60 |

out-of-focus images beyond about 9000 Å (probably because of optical limitations of the field-flattening lens) and because the spectrum is not perfectly parallel to the columns of the CCD. Instead, the spectra were extracted using software which first traces the position of the spectrum on an image by determining its centroid within a one-dimensional box down each row. Use of this algorithm to follow the curved spectra allowed minimization of the size of the extraction window, which decreased the effects of the night sky and thus improved the signal-to-noise ratio. The Seyfert galaxy spectra were then extracted over constant windows of 10–20 pixels (= 6″.6–13″.2), depending on the seeing and the extent of the object. The long-slit spectra of NGC 1976 with central wavelengths $\lambda$8960 and $\lambda$10200 were centered approximately 27″ east, 58″ north of $\theta_1$ Ori C = HD 37022, partly in one of the brightest regions and partly in the "dark bay," and they were summed over approximately 80 pixels = 53″. The two spectra with central wavelength $\lambda$7750, our first trial exposures on NGC 1976, were centered approximately 28″ west of this position and included only a small part of the bay.

The night-sky spectrum was determined by averaging several columns on both sides and spatially near the centroid positions of the object spectrum. This sky spectrum was then subtracted from the object spectrum. For the Orion Nebula, in which the nebular emission extended over the entire length of the slit, the sky spectrum was taken from a long exposure of NGC 4151 obtained during the same night (with the same instrumental setup) and scaled to remove all the sky lines observed in the sky + object spectrum as well as possible. The night sky is very bright in the near-IR at Lick Observatory, chiefly due to partly resolved OH emission bands, but with a continuum probably due to light pollution as well. This limited somewhat the identification and accurate measurement of the fluxes in the faintest emission lines in our program objects, despite the care taken in selecting the sky windows. Cosmic-ray events, which affect at most one or very occasionally two pixels, were identified visually and were removed and replaced by the mean of the surrounding pixels. They are easiest to identify in the background away from the spectrum. In the single high-resolution exposure of NGC 4151 centered at $\lambda$10200, however, a "larger" feature appears as an apparent line at $\lambda$10381, but close inspection shows it is close to but not coincident with the image of the nucleus. There is no trace of it on three exposures of this same spectral region taken in 1989 January, with the spectrograph rotated 180° in position angle. It must have been a "ghost" due to an internal reflection of some other line within the spectrograph. Because the sensitivity of the CCD is so low at the longest wavelengths, even weak ghosts of lines of shorter wavelength appear relatively strong if they occur in this region.

Two other ghosts, even more difficult to identify as such, appeared in the spectra of NGC 1976 at $\lambda$10406 and $\lambda$10870, the former quite strong. They are somewhat broader than the true nebular emission lines and can be seen to be apparently strongest in the region of the "dark bay" of NGC 1976, in contrast to the other lines, which are all strongest in the bright part of the nebula nearer the Trapezium stars. On repeat spectra of NGC 1976 taken in 1989 January, these two ghosts are slightly displaced (by about 4 Å in wavelength or 2 pixels on the CCD as measured directly on the raw data), establishing clearly that they are not true nebular lines (Osterbrock, Veilleux, and Tran 1990).

The spectra were calibrated in wavelength using comparison spectra of Hg-Ar, He, and Ne taken at the beginning and the end of each night, and additionally before and/or after each new grating rotation. To adjust the zero point of our wavelength scale to correct for instrument flexure, rather than using the night-sky lines, the standard Lick Observatory method for the visible spectral region (Osterbrock and Shaw 1988), we used the stronger identified emission lines in the galaxies themselves. A preliminary value of the zero point was determined with the aid of published heliocentric redshifts (Mazzarella and Balzano 1986; Dahari and De Robertis 1988) for these galaxies. Then, after the strongest lines in the object had been identified, improved values of the zero point correction and redshift, and, for the low-dispersion spectra, of the dispersion curve were found by differential corrections, choosing the best overall fits. The lines used in this process are marked with asterisks in the subsequent tables.

### *b) Flux Calibration*

The spectra were corrected for atmospheric extinction with the aid of mean extinction coefficients for Mount Hamilton. Molecular absorption bands of $O_2$ (the *A* band at 7620 Å) and $H_2O$ (bands in the regions 7100–7450 Å, 8100–8400 Å, and 8900–9900 Å) are also evident in the spectra, as illustrated in the raw spectrum of the standard star BD +17°4708 in Figure 1. They were removed separately from all of the observed spectra. These absorption bands are composed of many closely spaced absorption features, unresolved in our spectra. Many of

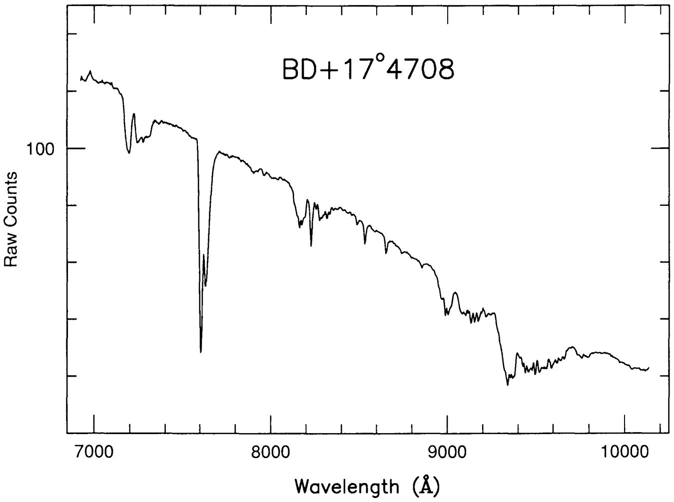


FIG. 1.—The unfluxed spectrum of BD +17°4708, illustrating the effects of the molecular absorption bands. The strong *A* band of $O_2$ is apparent between λλ7600–7700, and three regions of $H_2O$ bands are evident between λλ7100–7450, λλ8100–8400, and λλ8900–9900. Absorption lines at λλ8498, 8542, 8662 are Ca II lines in the stellar spectrum.

the features which comprise the *A* band are optically thick and therefore nearly independent of zenith distance, but most of those in the $H_2O$ bands are not. In order to correct for the effects of these absorption bands, the change in atmospheric transparency must be determined with zenith distance for each spectral channel. This was done by measuring the change in atmospheric transparency for a given infrared standard star observed at several different zenith distances throughout the night. (Obviously, it is best to observe standard stars as close in zenith distance and in time as possible to that of the program object to obtain the best correction.) However, the best absorption correction to use for an object was rarely exactly that inferred by interpolation for the program object. This probably results from the variation in strength of the absorption bands not only with zenith distance, but also with time. Furthermore, since the flux within the absorption bands is low, even for bright standard stars, the absorption correction as a function of zenith distance is necessarily poorly determined.

The following technique was adopted for correcting for the atmospheric absorption bands. Just before and/or after observing each program object, a high signal-to-noise spectrum of a standard star from Oke and Gunn (1983) was obtained at comparable zenith distance. The strength and the profile of the atmospheric absorption bands were determined for each of the standard stars by linearly interpolating the continuum over the spectral regions of the four bands. These interpolated spectra were then divided by the original spectra to produce absorption correctors—i.e., functions of wavelength which are equal to unity everywhere except at the positions of the absorption bands, where they are larger. Due to flexure of the telescope, the absorption correctors obtained from the stars sometimes had to be shifted in wavelength by a fraction of a channel to best correct the galaxy spectrum (especially for the *A* band).

The best absorption corrector for each program object was determined empirically. It was not necessarily the one determined from the standard star closest to the object's zenith distance, nor even a linear combination of the absorption correctors from standard stars with zenith distances bracketing that of the object. Once the absorption corrector for a given program object was selected, its amplitude at each of the four absorption bands was varied independently, using a different scaling factor for each band. The best scaling factors were determined by multiplying the object spectrum by the corrector and judging the smoothness of the resulting continuum in the object's spectrum at the positions of the absorption bands.

This method seems to work better than a formal solution of the atmospheric transparency at each wavelength, and it is certainly better than a simple division of the object spectrum by that of a star obtained at similar zenith distance. It allows more flexibility in the determination of the strength of the absorption features and does not introduce any spurious emission lines in the object spectrum at the position of absorption lines in the standard star. Note, however, that this method only allows for differences in the zenith distance dependence of the strengths of entire atmospheric bands while, in reality, the strength of each of the individual lines constituting the bands scales differently with zenith distance (depending on their optical depths). Obviously, the available spectral resolution is not sufficient to measure the absorption lines individually, and the method described above is therefore a good compromise.

Finally, the spectra were calibrated approximately on a relative flux scale using our atmospherically corrected spectra of the standard stars. The spectra were converted to flux units using a mean nightly response curve for each grating rotation. The absolute near-IR flux is very uncertain due to temporal variations in seeing, passing clouds, and humidity; the relative flux should be somewhat more accurate, although this accuracy declines longward of 8900 Å due to the larger amplitude of the atmospheric correction, the effects of the field-flattening lens, and the decreasing sensitivity of the CCD. The three sections of the NGC 1976 high-dispersion spectrum were brought to the same relative-intensity scale by matching the strongest lines in the regions of overlap between successive sections. For the three sections of the NGC 4151 high-dispersion spectrum, the overall relative-intensity scale was set by matching the relative intensities of the strongest lines in each section to those in the previously reduced normal dispersion spectrum, which extends over all three sections.

### *c) Relative Emission-Line Fluxes*

The fluxes in the various emission lines were measured for each digital spectrum with a software package available at Lick Observatory described by Osterbrock and Shaw (1988). Briefly, the line fluxes were measured either by being fitted with one or more Gaussians, or by having the flux integrated directly above an eye-estimated continuum level. As mentioned above, the long-slit images are somewhat degraded longward of about 9000 Å, so that the emission-line profiles at the longest wavelengths tended to be non-Gaussian. Hence, the direct integrations rather than the Gaussian fits were usually chosen, although Gaussians were used to deconvolve nearly blended lines. To check the two methods for consistency, the flux in each line was measured using both techniques. For strong, isolated lines, the two methods give the same flux to within about 5%; the direct integrations give the best results for lines with profiles which deviate greatly from Gaussian ones (e.g., the broad wings of [S III] λ9531), while the Gaussian fits work best for partly blended lines. In the latter case, the individual fluxes were scaled by the sum of the fluxes measured by direct integration.

The data for the Orion Nebula, NGC 1976, are presented in Table 2. Listed in order are the identification, including ion

TABLE 2

NGC 1976: Wavelengths, Identifications, and Relative Line Intensities

| Ion | Multiplet | $\lambda_m$ | $\lambda_0$ | $I_\lambda/I(\lambda 7324)$ | $I_\lambda/I(\lambda 9069)$ |
|---|---|---|---|---|---|
| O I | (21) | 7002.7 | 7002.0 | 0.62 | 0.14 |
| He I | (10) | 7065.0 | 7065.3 | 61 | 13 |
| [Ar III] | (1 F) | 7134.6 | 7135.8 | 135 | 31 |
| C II | (3) | 7239.8 | 7236.2 | 2.4 | 0.55 |
| O I | (20) | 7254.0 | 7254.4 | 0.96 | 0.22 |
| He I | (45) | 7281.5 | 7281.3 | 6.0 | 1.4 |
| ? | ... | 7298.1 | ... | 0.37 | 0.08 |
| [O II] | (2 F) | 7320.1 | 7319.6 | 55 | 13 |
| [O II] | (2 F) | 7330.4 | 7330.2 | 45 | 10 |
| [Ni II] | (2 F) | 7378.0 | 7377.8 | 0.69 | 0.16 |
| [Ni II] | (2 F) | 7411.5 | 7411.6 | 0.23 | 0.05 |
| ? | ... | 7442.0 | ... | 0.19 | 0.04 |
| [Fe II] | (14 F) | 7452.5 | 7452.5 | 0.16 | 0.04 |
| N I | (3) | 7470.5 | 7468.3 | 0.41 | 0.09 |
| ? | ... | 7500.0 | ... | 0.37 | 0.08 |
| [Ar III] | (1 F) | 7752.0 | 7751.1 | 34 | 7.7 |
| He I | (69) | 7817.7 | 7816.2 | 0.50 | 0.11 |
| [Ni III] | (1 F) | 7889.1 | 7889.9 | 0.68 | 0.15 |
| H I | Pa 20 | 8392.2 | 8392.4 | 3.2 | 0.72 |
| H I | Pa 19 | 8413.3 | 8413.3 | 3.2 | 0.72 |
| H I | Pa 18 | 8438.3 | 8438.0 | 3.7 | 0.85 |
| O I | (4) | 8446.2 | 8446.4 | 11 | 2.6 |
| H I | Pa 17 | 8467.4 | 8467.3 | 4.6 | 1.0 |
| H I | Pa 16 | 8502.5 | 8502.5 | 5.3 | 1.2 |
| ? | ... | 8520.4 | ... | 0.26 | 0.06 |
| ? | ... | 8529.2 | ... | 0.28 | 0.06 |
| H I | Pa 15 | 8545.2 | 8545.4 | 6.2 | 1.4 |
| [Cl II] | (1 F) | 8577.3 | 8578.7 | 1.8 | 0.42 |
| H I | Pa 14 | 8598.4 | 8598.4 | 7.7 | 1.7 |
| [Fe II] | (13 F) | 8617.4 | 8617.0 | 0.54 | 0.12 |
| ? | ... | 8648.8 | ... | 0.25 | 0.06 |
| H I | Pa 13 | 8664.9 | 8665.0 | 9.5 | 2.2 |
| N I | (1) | 8683.0 | 8681.6 | 0.75 | 0.17 |
| N I | (1) | 8703.6 | 8703.2 | 0.13 | 0.03 |
| N I | (1) | 8711.1 | 8711.7 | 0.16 | 0.04 |
| ? | ... | 8732.7 | ... | 0.49 | 0.11 |
| H I | Pa 12 | 8751.0 | 8750.5 | 12 | 2.7 |
| ? | ... | 8765.8 | ... | 0.25 | 0.06 |
| ? | ... | 8777.7: | ... | 0.74 | 0.17 |
| H I | Pa 11 | 8863.4 | 8862.8 | 16 | 3.6 |
| H I | Pa 10 | 9015.4 | 9014.9 | 16 | 3.6 |
| [S III] | (1 F) | 9069.0 | 9069.0 | 442 | 100 |
| H I | Pa 9 | 9228.8 | 9229.0 | 33 | 7.5 |
| ? | ... | 9295.0 | ... | 24 | 5.3 |
| [S III] | (1 F) | 9528.8: | 9530.9 | 1426 | 322 |
| H I | Pa 8 | 9549.1: | 9546.0 | 147 | 33 |
| ? | ... | 9700.0 | ... | 0.95 | 0.22 |
| ? | ... | 9719.4 | ... | 0.92 | 0.21 |
| ? | ... | 9738.4 | ... | 0.90 | 0.2 |
| ? | ... | 9754.4 | ... | 10 | 2.3 |
| [C I] | (1 F) | 9822.4 | 9824.1 | 0.45 | 0.10 |
| [C I] | (1 F) | 9850.4 | 9850.3 | 1.3 | 0.30 |
| ? | ... | 9890.5 | ... | 1.2 | 0.27 |
| ? | ... | 9903.4 | ... | 0.59 | 0.13 |
| He I | (85) | 10027.0: | 10031.2 | 11 | 2.4 |
| H I | Pa 7 | 10049.3 | 10049.4 | 86 | 19.0 |
| [S II] | (3 F) | 10286.5 | 10286.7 | 2.0 | 0.46 |
| [S II] | (3 F) | 10320.4 | 10320.5 | 3.5 | 0.79 |
| ? | ... | 10329.1 | ... | 2.1 | 0.48 |
| [S II] | (3 F) | 10335.4 | 10336.4 | 2.8 | 0.64 |
| He I | (1) | 10830.8 | 10830.2 | 636 | 144 |
| H I | Pa 6 | 10938.4 | 10938.1 | 102 | 23 |
| ? | ... | 10950.5 | ... | 16 | 3.5 |

and multiplet number from the RMT (Moore 1945), the measured wavelength, the rest wavelength of the identified line, and the relative line fluxes, normalized first by the sum of the [O II] lines ($F[\lambda 7320 + \lambda 7330] = F[\lambda 7324] = 100$), and then by the weaker [S III] line ($F[\lambda 9069] = 100$). We chose the former scaling because the system response is better determined at the blue end of our spectral range (see the previous subsection), but we also include the latter scaling in order to compare these strengths directly with those in the Seyfert galaxies in which [O II] λ7324 was not always measured. Note that the fluxes are the observed values and are not corrected for interstellar extinction. The identifications are discussed in the next section. Note that though the multiplet numbers are from Moore (1945), the most accurate wavelengths currently available were used, chiefly from Bowen (1960), Mendoza (1983), and other sources listed by Osterbrock (1989). The high-dispersion data for the bright Seyfert galaxy NGC 4151 are presented in Table 3 in the same manner as for NGC 1976. The line identifications for NGC 4151 are also discussed in § III.

The low-dispersion spectra of the Seyfert galaxies were reduced and measured as described above. The measured rest wavelengths of the unidentified emission lines are thus on the system of the stronger identified lines used in the reduction and marked by asterisks in Table 4. Note in particular that the [O II] λλ7320, 7330 doublet, which is unresolved at this dispersion but reasonably strong in nearly all these Seyfert galaxies, was treated as an *unidentified* line in this reduction, and its effective wavelength was thus measured. Likewise, O I λ8446, which is a single line (actually an extremely close triplet that cannot be resolved because of velocity broadening), was treated in the same way. Thus the wavelengths of these lines given in Table 4 are the measured wavelengths in the rest systems defined by the other emission lines listed in these galaxies, while for the (other) identified lines, the wavelengths given are the "laboratory" wavelengths used. These identifications are discussed further in § III. The last column gives the measured relative flux in each line, normalized to $F(\lambda 9069) = 100$. This normalization was used because the [S III] lines are among the few that are present in all the galaxies, and λ9069 is closer to the center of the spectral region observed.

The low-dispersion spectra of four of the galaxies listed in Table 1, NGC 1320, I Zw 1, II Zw 136, and VII Zw 31, were reduced as described above, but two of them were not measured in the same way and the results for the other two were not tabulated in this way. They are all special cases and are discussed separately in § IV.

## III. LINE IDENTIFICATIONS

### *a*) *NGC 1976*

The measured wavelengths, identifications, and relative fluxes for the Orion Nebula are listed in Table 2. The three

TABLE 3

NGC 4151: Wavelengths, Identifications, and Relative Line Intensities

| Ion | Multiplet | $\lambda_m$ | $\lambda_0$ | $I(\lambda)/I(\lambda 7324)$ | $I(\lambda)/I(\lambda 9069)$ |
|---|---|---|---|---|---|
| [Ar V] | (1 F) | 7005.4* | 7005.7 | 11 | 5.7 |
| ? | ... | 7047.3 | ... | 8.2 | 4.3 |
| He I | (10) | 7065.1* | 7065.3 | 16 | 8.5 |
| [Ar III] | (1 F) | 7135.5* | 7135.8 | 75 | 40 |
| [Fe II] | (14 F) | 7152.9 | 7155.1 | 25 | 13 |
| [Fe II] | (14 F) | 7170.3 | 7172.0 | 17 | 9 |
| [O II] | (2 F) | 7319.6* | 7319.9 | 57 | 30 |
| [O II] | (2 F) | 7330.2* | 7330.2 | 43 | 22 |
| [Ni II] | (2 F) | 7377.3* | 7377.8 | 18 | 9.2 |
| [Ni II] | (2 F) | 7402.7* | 7401.8 | 3.0 | 1.6 |
| [Fe II] | (14 F) | 7452.6 | 7452.5 | 4.4 | 2.3 |
| [Ar III] | (1 F) | 7751.7* | 7751.1 | 22 | 12 |
| ? | ... | 7767.8 | ... | 3.6 | 1.9 |
| [Fe XI] | (1 F) | 7891.1 | 7891.8 | 9.3 | 5.0 |
| He II | (6) | 8237.6* | 8236.8 | 8.9 | 4.7 |
| [Cl II] | (1 F) | 8578.9* | 8578.7 | 3.0 | 1.6 |
| [Fe II] | (13 F) | 8618.0 | 8616.9 | 25 | 13 |
| ? | ... | 8854.5 | ... | 10 | 5.4 |
| [Fe II] | (13 F) | 8893.9 | 8891.9 | 7.3 | 3.9 |
| [S III] | (1 F) | 9068.6* | 9068.9 | 189 | 100 |
| ? | ... | 9198.0 | ... | 13 | 7.0 |
| H I | Pa 9 | 9229.0* | 9229.0 | 17 | 8.9 |
| [S III] | (1 F) | 9530.9* | 9531.8 | 593 | 313 |
| [C I] | (1 F) | 9851.5 | 9850.3 | 7.3 | 3.8 |
| [S VIII] | (1 F) | 9911.4 | 9911 | 10 | 5.3 |
| ? | ... | 10021.1 | ... | 8.4 | 4.4 |
| H I | Pa 7 | 10048.4* | 10049.4 | 21 | 11 |
| ? | ... | 10127.2 | ... | 30 | 16 |
| [S II] | (3 F) | 10288.7 | 10286.7 | 13 | 6.9 |
| [S II] | (3 F) | 10320.3 | 10320.5 | 19 | 10 |
| ? | ... | 10598.2 | ... | 19.3 | 11 |
| ? | ... | 10795.7 | ... | 48.5 | 27 |
| He I | (1) | 10832.7* | 10830.3 | 353 | 194 |
| ? | ... | 10855.9 | ... | 107 | 59 |
| H I | Pa 6 | 10935.4* | 10938.1 | 53 | 29 |

TABLE 4

WAVELENTHS, IDENTIFICATIONS, AND RELATIVE INTENSITIES IN SEYFERT GALAXIES

| λ | Ion | Multiplet | $I(\lambda)/I(\lambda9069)$ |
|---|---|---|---|
| **NGC 3227** | | | |
| 7135.8* | [Ar III] | (1 F) | 9 |
| 7324.0 | [O II] | (2 F) | 20 |
| 7377.8* | [Ni II] | (2 F) | 4 |
| 8448.7 | O I | (4) | 75 |
| 9068.9* | [S III] | (1 F) | 100 |
| 9135.1 | ... | ... | 27 |
| 9189.3 | ... | ... | 27 |
| 9530.9* | [S III] | (1 F) | 255 |
| **NGC 3516** | | | |
| 7054.3 | ... | ... | 21 |
| 8416.1 | ... | ... | 38 |
| 8453.7 | O I | (4) | 11 |
| 9068.9* | [S III] | (1 F) | 100 |
| 9144.0 | ... | ... | 109 |
| 9192.1 | ... | ... | 32 |
| 9530.9* | [S III] | (1 F) | 197 |
| **NGC 4051** | | | |
| 7065.3* | He I | (10) | 88 |
| 7135.8* | [Ar III] | (1 F) | 16 |
| 7325.2 | [O II] | (2 F) | 29 |
| 7866.9 | ... | ... | 10 |
| 7889.0 | [Fe X] | (1 F) | 44 |
| 8449.4 | O I | (4) | 199 |
| 9068.9* | [S III] | (1 F) | 100 |
| 9208.0 | λ9212 | ... | 115 |
| 9530.9* | [S III] | (1 F) | 305 |
| **NGC 4151** | | | |
| 7005.9 | [Ar V] | (1 F) | 7 |
| 7065.3* | He I | (10) | 16 |
| 7135.8* | [Ar III] | (1 F) | 40 |
| 7324.1 | [O II] | (2 F) | 52 |
| 7377.8* | [Ni II] | (2 F) | 7 |
| 7453.2 | [Fe II] | (14 F) | 3 |
| 7751.1* | [Ar III] | (1 F) | 10 |
| 7865.9 | ... | ... | 3 |
| 7888.7 | [Fe XI] | (1 F) | 6 |
| 8429.8 | O I | (4) | 21 |
| 8618.1 | [Fe II] | (13 F) | 6 |
| 9068.9* | [S III] | (1 F) | 100 |
| 9530.9* | [S III] | (1 F) | 271 |
| 9850.3* | [C I] | (1 F) | 2 |
| 9913.2 | [S VIII] | (1 F) | 4 |
| 10049.4* | H I | Pa 7 | 6 |
| **NGC 6814** | | | |
| 8407.2 | ... | ... | 38 |
| 9068.9* | [S III] | (1 F) | 100 |
| 9166.2 | ... | ... | 25 |
| 9530.9* | [S III] | (1 F) | 315 |
| **NGC 7469** | | | |
| 7065.3* | He I | (10) | 55 |
| 7135.8* | [Ar III] | (1 F) | 14 |
| 7322.6 | [O II] | (2 F) | 24 |
| 7377.8* | [Ni II] | (2 F) | 7 |
| 8439.8 | O I | (4) | 64 |
| 8472.8 | ... | ... | 41 |
| 9068.9* | [S III] | (1 F) | 100 |
| 9206.7 | λ9212 | ... | 215 |
| 9530.9* | [S III] | (1 F) | 341 |
| **Mrk 1** | | | |
| 7005.7* | [Ar V] | (1 F) | 3 |
| 7065.3* | He I | (10) | 12 |
| 7135.8* | [Ar III] | (1 F) | 36 |
| 7323.4 | [O II] | (2 F) | 65 |
| 7377.8* | [Ni II] | (2 F) | 8 |
| 7751.0* | [Ar III] | (1 F) | 7 |
| 9068.9* | [S III] | (1 F) | 100 |
| 9530.9* | [S III] | (1 F) | 253 |
| **Mrk 3** | | | |
| 7098.8 | ... | ... | 5 |
| 7135.8* | [Ar III] | (1 F) | 26 |
| 7325.4 | [O II] | (2 F) | 37 |
| 7377.8* | [Ni II] | (2 F) | 5 |
| 7751.1* | [Ar III] | (1 F) | 6 |
| 8832.1 | ... | ... | 3 |
| 8855.6 | ... | ... | 2 |
| 8951.8 | ... | ... | 1 |
| 9068.9* | [S III] | (1 F) | 100 |
| 9530.9* | [S III] | (1 F) | 203 |
| **Mrk 915** | | | |
| 7005.7* | [Ar V] | (1 F) | 13 |
| 7035.4 | ... | ... | 12 |
| 7065.3* | He I | (10) | 13 |
| 7135.8* | [Ar III] | (1 F) | 33 |
| 7322.7 | [O II] | (2 F) | 24 |
| 7377.8* | [Ni II] | (2 F) | 5 |
| 7751.1* | [Ar III] | (1 F) | 11 |
| 7863.9 | ... | ... | 5 |
| 7889.9* | [Ni III] | (1 F) | 6 |
| 9014.8 | H I? | Pa 10? | 12 |
| 9068.9* | [S III] | (1 F) | 100 |
| 9530.9* | [S III] | (1 F) | 289 |
| **Mrk 993** | | | |
| 8828.9 | ... | ... | 22 |
| 8849.0 | ... | ... | 47 |
| 9043.1 | ... | ... | 34 |
| 9068.9* | [S III] | (1 F) | 100 |
| 9530.9* | [S III] | (1 F) | 149 |
| **Mrk 1126** | | | |
| 7116.4 | ... | ... | 13 |
| 7135.8* | [Ar III] | (1 F) | 18 |
| 7862.9 | ... | ... | 9 |
| 7893.2 | [Fe XI] | (1 F) | 25 |
| 9068.9* | [S III] | (1 F) | 100 |
| 9134.2 | ... | ... | 26 |
| 9530.9* | [S III] | (1 F) | 194 |
| **III Zw 77** | | | |
| 7135.8* | [Ar III] | (1 F) | 31 |
| 7322.2 | [O II] | (2 F) | 72 |
| 7865.1 | ... | ... | 61 |
| 7891.8* | [Fe XI] | (1 F) | 139 |
| 8452.3 | O I | (4) | 172 |
| 9068.9* | [S III] | (1 F) | 100 |
| 9221.4 | λ9212 | ... | 310 |
| 9530.9* | [S III] | (1 F) | 397 |
| 9690.3 | ... | ... | 50 |

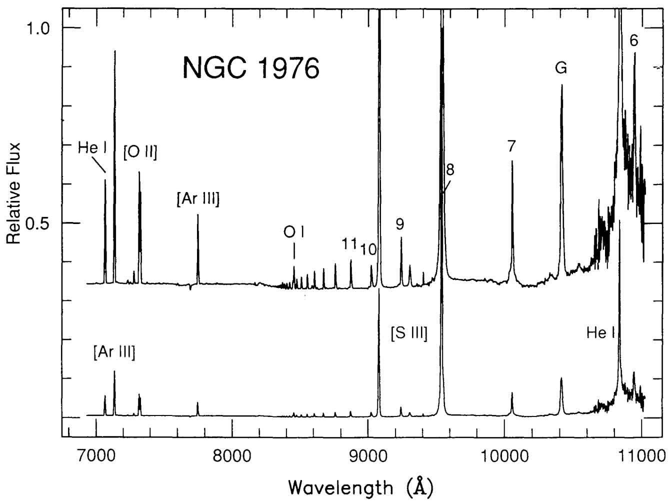


FIG. 2.—The near-infrared spectrum of NGC 1976, λλ6950–11000, in the rest system of the object. The feature marked "G" at λ10406 and the weaker feature at λ10870 are ghosts, not true nebular emission lines.

long-exposure spectra have been combined to form one composite spectrum, extending from below λ7000 to just above λ11000, as shown in Figure 2. The strongest lines can easily be recognized on the lower, normal-scale plot. The Paschen series is particularly apparent in the upper, enlarged plot, where it can be seen from the progression of intensities that the atmospheric absorption was not removed from Pa 10 completely correctly. Also, the poorer signal-to-noise ratio in the data above about λ10500, resulting from the steeply decreasing sensitivity of the CCD, is quite evident. The apparent wings on He I λ10830 are clearly not real, but they result from the poorer definition in this region mentioned in the previous section plus the very low sensitivity.

Previous line identification lists for NGC 1976 which reach appreciably into the near-infrared include Morgan (1971), Grandi (1975*b*), and Kaler (1976). Out to about λ8400, Grandi (1975*b*) was able to record quite a few lines that are too faint to measure on our spectra, but longward of about λ9500, we have observed a fair number of lines apparently not previously reported in NGC 1976, many of them still unidentified.

This spectrum of NGC 1976 is very helpful for comparison with the spectra of Seyfert galaxies, at least for low-ionization lines. Note in particular that our measurements confirm several rather faint [Fe II] lines and two [Ni II] lines previously identified by Morgan (1971) and Grandi (1975*b*). The lines seen are those expected from the best available transition probabilities, except that we seem to have measured the weak [Ni II] λ7412 as stronger than it is predicted to be (Garstang 1962; Nussbaumer and Storey 1980, 1982, 1988; Henry 1987), but in fairly good agreement with an estimate from a published very high signal-to-noise ratio scan of this very wavelength region (Henry and Fesen 1988). On the other hand, the [S II] λλ10287, 10320, 10336 lines, though weak, seem to have relative intensities approximately in accord with those predicted using the best available collision strengths and transition probabilities for this ion. The fourth component, not detected on our spectrum, is predicted to be still weaker (De Robertis, Dufour, and Hunt 1987). The identification of the four N I lines of multiplet (1) (λ8681.6 is a blend of a close pair), suggested by the referee, Simon L. Morris, further confirms the resonance-fluorescence predictions (Grandi 1975*a*) and observations of the strongest lines of multiplets (2) and (3) of Grandi 1975*b*).

### *b*) *NGC 4151*

The measured wavelengths, identifications, and relative fluxes for the high-ionization Seyfert 1.5 galaxy NGC 4151 are listed in Table 3. The long-exposure spectra, de-redshifted to the rest system of the object, have been combined to form one composite spectrum, as shown in Figure 3. The poorer signal-to-noise ratio, resulting from the faintness of NGC 4151 relative to NGC 1976, is evident, and the seriousness of this problem at the longest wavelengths is apparent near He I λ10830. The straight-line segment near λ10381 marks the spot from which a flaw was removed. Many of the stronger lines in the near-infrared spectrum of NGC 4151 have been previously identified by Andrillat and Collin-Souffrin (1975) and Boksenberg *et al.* (1975). For identifying the fainter lines, several papers on near-infrared spectra of supernova remnants by Dennefeld (1982, 1986) and Dennefeld and Pequignot (1983) proved especially useful.

As in NGC 1976, several [Fe II] and two [Ni II] emission lines are confirmed. [C I] λ9850 and [Cl II] λ8579 are definitely present; in each case, the transition probabilities show that the next strongest lines [C I] λ9824 and [Cl II] λ9124 are expected to be too faint to be detectable on these spectra (Mendoza 1983).

The identification of [Fe XI] λ7892 is quite certain, because this line is observed in many high-ionization Seyfert galaxies and its strength is well correlated with that of [Fe XI] λ6375; both in turn are well correlated with the strength of [Fe VII] λ6087 (Grandi 1978). The suggested identification of λ9911 with [S VIII] $2p^5\,^2P_{3/2}$–$2p^5\,^2P_{1/2}$ is plausible but more speculative. This line is observed in the solar corona (Svensson, Ekberg, and Edlen 1974), but it is the only optical or near-infrared line of this ion. The ionization potential of $S^{+6}$ (which must be ionized to $S^{+7}$ to produce the [S VIII] spectrum) is 281 eV, while the ionization potentials of $Fe^{+8}$ and $Fe^{+9}$ are 234 eV and 262 eV, respectively. On the other hand, to ionize $Fe^{+12}$ requires 361 eV, and [Fe XIV] has not been observed in NGC 4151 or any other Seyfert galaxy nuclei except III Zw 77, while to ionize $S^{+7}$ requires 330 eV. Thus, it is quite plausible

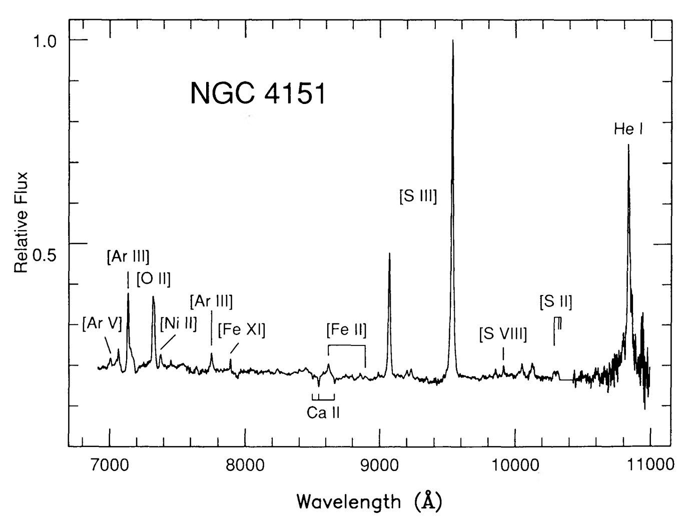


FIG. 3.—The near-infrared spectrum of NGC 4151, λλ6950–11000, in the rest system of the object.

to suppose that $S^{+7}$ is present and emits [S VIII] λ9911 in the same regions, near the active nucleus, in which $Fe^{+9}$ and $Fe^{+10}$ are present and emit [Fe X] λ6375 and [Fe XI] λ7892 (Korista and Ferland 1989).

### *c) Other Seyfert Galaxies*

The measured wavelengths, identifications, and relative fluxes from the "normal-dispersion" spectra of 12 Seyfert galaxies are listed in Table 4, and the spectra of two of these objects are shown in Figures 4 and 5. The identifications are based on the papers previously mentioned. As stated in § II, the wavelengths marked with an asterisk are laboratory wavelengths of well-identified lines that were used to obtain the final best wavelengths listed for all the other lines. It is difficult to estimate the accuracy of this process. For the lines used in establishing the final best wavelengths, the "corrections" that would be read from the curves if they were regarded as unknown lines (the errors that would result in their final wavelengths) range from 0.0 to 3.8 Å, with a mean of 0.9 Å and a median of 0.7 Å, both without regard to sign. The average error for an unknown line is clearly larger than either of these last two numbers. In the normal-dispersion spectrum of NGC 4151, three lines that were not used in establishing the final wavelengths, but were later identified have errors in measured wavelength ranging from 0.2 Å to 1.2 Å, with root mean square 0.8 Å. Probably the wavelengths of the unidentified lines, if they are real, are of order ±2 Å, since they are mostly fainter and not as well defined as the identified lines.

The [O II] λλ7320, 7330 doublet was measured as a blend in eight of these Seyfert galaxies. The mean wavelength determined from these objects for the blend is 7323.7 ± 0.5 Å. The calculated value, which depends only slightly on electron density for $N_e \leq 10^6$ cm$^{-3}$, is 7324.2 Å, using the best nebular wavelength measurements (Barnett and McKeith 1988). Either of these are good values to use for any spectrograph or scanner in which this doublet is not resolved. The mean measured wavelength of the broad O I line in the six Seyfert galaxies which show it on our spectra as 8445.6 ± 3.7 Å, while the laboratory value is 8446.5.

[Fe XI] λ7892 was measured in three of these galaxies in which it was not used to fix the final wavelengths. The mean measured wavelength in these three objects is 7890.3 ± 1.5 Å, which differs from the wavelength 7891.8 (Svensson, Ekberg, and Edlen 1974) by −1.5 ± 1.5 Å. This is an average blueshift smaller than the average −5.6 ± 1.6 Å found by Grandi (1978) for this line in seven Seyfert galaxies. It is impossible to distinguish [Fe XI] λ7892 with a typical blueshift from [Ni III] λ7890 by the measured wavelength alone; the distinction must be made on the basis of the presence and strengths of [Fe VII] λ6087 and [Fe X] λ6375 elsewhere in the spectra and the general correlation of the presence and strengths of these three high-ionization lines (Grandi 1978). We have tentatively identified [Ni III] λ7890 in the spectrum of Mrk 915, which has moderate [Fe VII] λ6087 and weak but definite [Fe X] λ6375, but the observed line may in fact be [Fe XI].

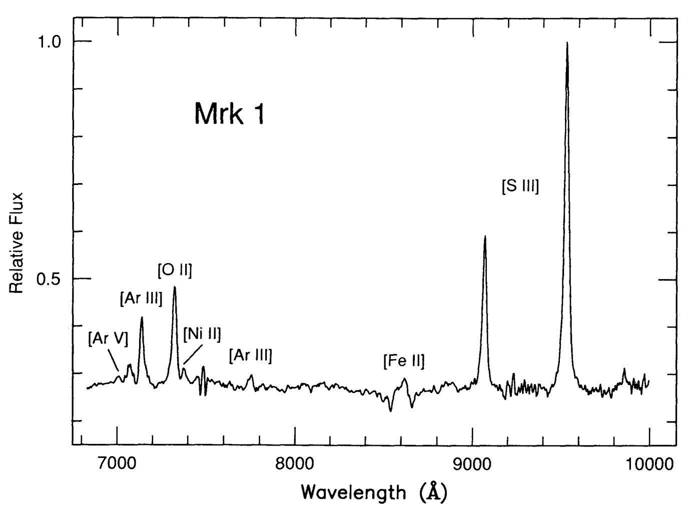


FIG. 4.—The near-infrared spectrum of Mrk 1, λλ7000–10000, in the rest system of the object.

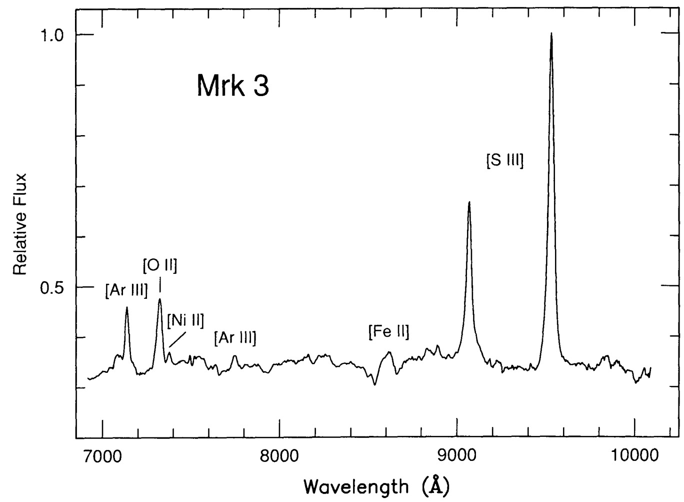


FIG. 5.—The near-infrared spectrum of Mrk 3, λλ7000–10000, in the rest system of the object.

The "λ9212" feature, identified in three of these objects (NGC 4051, NGC 7469, and III Zw 77), has been previously discussed by Persson and McGregor (1985), as "λ9229," and by Morris and Ward (1989) as "λ9210." It is clearly not Pa 9 alone, for both Pa 8 and Pa 10 are much weaker than it. It is probably a complex blend of Pa 9 with several lines of other atoms and ions as discussed by these authors. Its wavelength is not well defined even to ±1 Å on our spectra (we tried to measure the apparent center of the top 80% of the profile), and the mean is 9212 ± 5 Å. The line has quite different widths in different objects, confirming that it is a blend of lines whose relative intensities are not always the same. Note, however, that the spectral region is considerably affected by a strong $H_2O$ absorption feature. Part of the structure in the "λ9212" feature can originate from an imperfect atmospheric correction.

Five of these galaxies have an apparent emission line near λ7865; its mean wavelength from these objects is λ7864.9 ± 0.7. All the galaxies in which it appears have relatively high ionization. Inspection of the spectra at high magnification shows it is probably a true unidentified line, but it may conceivably be a blue wing of [Fe XI] with similar structure in all three objects. Two other emission lines that apparently appear in two or more of these galaxies are λ9191.0 ± 1.7 (in two) and λ9138.0 ± 3.4 (in three). The former appears more likely to be a genuine line than the latter.

## IV. OTHER GALAXIES

### a) I Zw 1

The near-infrared spectrum of I Zw 1, de-redshifted to the rest system of the object using $z = 0.0603$ (see below), is shown in Figure 6. It is quite different in appearance from most of the other Seyfert galaxy spectra considered here, and in particular, the [S III] λλ9069, 9531 are either absent or very weak. The optical spectrum of I Zw 1 is known to be dominated by Fe II emission lines originating in upper levels connected with the ground term and other low-lying terms by permitted radiative transitions (Sargent 1968; Phillips 1976). Phillips (1976) identified some of the members of Fe II multiplet (73) in emission in the near-infrared spectrum of I Zw 1 (as indicated in his Fig. 1), and also the [Ca II] $4\,^2S$–$3\,^2D$ λλ7291, 7324 doublet. Persson and McGregor (1985) identified two Fe II lines of multiplet (73), O I λ8446, and the Ca II $3\,^2D$–$4\,^2P$ λλ8498, 8542, 8662 multiplet in emission. The O I and Ca II lines are very well shown in Figure 1 of Persson (1988).

The emission lines in I Zw 1 are severely blended. We therefore did not try to define a continuum and measure relative intensities, but instead measured only the wavelengths of the peaks of the various features as well as they could be defined. The wavelength zero point was provided by a comparison-lamp spectrum taken at approximately the same hour angle and declination, twenty minutes before the exposure of the galaxy began. The results are listed in Table 5. Note that they are given to the nearest 1 Å, which is all the accuracy justified except for the two [Ca II] lines. Our spectra confirm all the identifications listed above and add Fe II λ7462 of multiplet (73). The five strongest lines of this multiplet are now accounted for in I Zw 1, all those with laboratory intensities ≥12 in the RMT, two of them blended with [Ca II] and the other three identified. The other members of the multiplet, with laboratory intensities ≤8, are not seen. This is the only Fe II multiplet in this spectral region whose upper levels, like the other Fe II multiplets observed in the optical spectral region, are connected with the ground and other low terms by strong permitted transitions, indicating excitation by resonance fluorescence and/or collisional excitation, with subsequent scattering and fluorescence with large optical depths (Phillips 1978*a*; Netzer and Wills 1983).

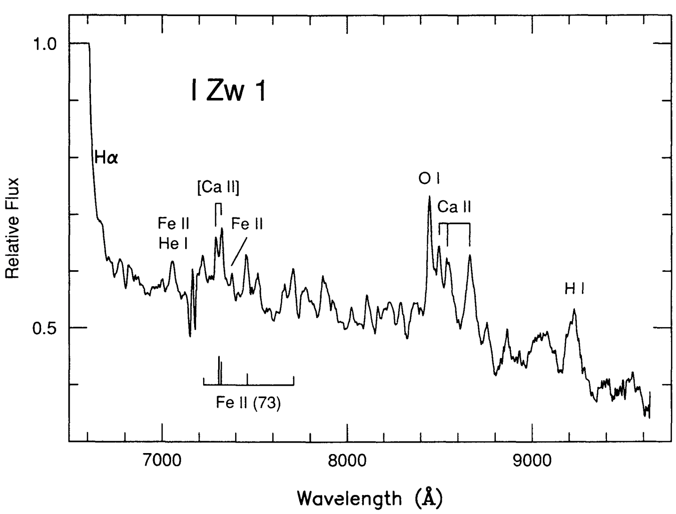


FIG. 6.—The near-infrared spectrum of I Zw 1, λλ6750–9500, in the rest system of the object.

TABLE 5

I Zw 1: WAVELENGTHS, IDENTIFICATIONS, AND REDSHIFTS

| MEASURED $\lambda_m$ | IDENTIFICATION Ion | Multiplet | REST $\lambda_0$ | $z$ |
|---|---|---|---|---|
| 7423 | ... | ... | 7000.8 | ... |
| 7483 | He I | (10) | 7065.3 | 0.0591 |
| | Fe II | unclassified | 7067.4 | 0.0588 |
| 7658 | Fe II | (73) | 7224.5 | 0.0600 |
| 7734 | [Ca II] | (1 F) | 7291.5 | 0.0607 |
| | Fe II | (73) | 7308.0 | 0.0583 |
| 7768 | [Ca II] | (1 F) | 7323.9 | 0.0606 |
| | Fe II | (73) | 7320.7 | 0.0611 |
| 7826 | Fe II | unclassified | 7376.5 | 0.0609 |
| 7911 | Fe II | (73) | 7462.4 | 0.0601 |
| 7975 | ... | ... | 7521.6 | ... |
| 8127 | ... | ... | 7665.0 | ... |
| 8175 | Fe II | (73) | 7711.7 | 0.0601 |
| 8230 | ... | ... | 7762.1 | ... |
| 8239 | ... | ... | 7770.6 | ... |
| 8344 | ... | ... | 7869.6 | ... |
| 8359 | ... | ... | 7883.8 | ... |
| 8508 | ... | ... | 8024.3 | ... |
| 8600 | ... | ... | 8111.1 | ... |
| 8662 | ... | ... | 8169.5 | ... |
| 8793 | ... | ... | 8293.1 | ... |
| 8958 | O I | (4) | 8446.5 | 0.0606 |
| 9012 | Ca II | (2) | 8498.0 | 0.0605 |
| 9055 | Ca II | (2) | 8542.1 | 0.0600 |
| 9188 | Ca II | (2) | 8662.1 | 0.0607 |
| 9283 | ... | ... | 8755.2 | ... |
| 9786 | λ9212 | ... | 9229.5 | ... |

In addition, two other Fe II near-infrared emission lines can apparently be identified in I Zw 1, λλ7067, 7376 (although the former may instead be He I λ7065). They are two of the strongest unclassified Fe II lines listed in the RMT and the only two in this spectral region. If these identifications are correct, they suggest that the upper levels of these two lines belong among the low even terms of Fe II, as do the upper levels of all the other lines of this ion observed in I Zw 1.

All these identified lines are listed in Table 5, along with the measured redshift of each. The mean redshift derived from all of them, $z = 0.0603 \pm 0.0002$, was used to calculate the rest wavelengths of the other apparent features measured, some of which are probably unidentified lines while others are no doubt blends or artifacts of the reduction process. Note that we have determined, using this redshift, the rest wavelength λ9229.5 for the feature we have called λ9212, nearly identical with the rest wavelength measured by Persson and McGregor (1985). Some remarks on the astrophysical implications of the observed emission-line spectrum of I Zw 1 are included in § V.

### b) II Zw 136

II Zw 136 has a near-infrared emission-line spectrum somewhat similar to that of I Zw 1 but with a somewhat larger redshift ($z = 0.0615$), considerably broader and somewhat weaker Fe II lines, and weak but definitely present forbidden lines. The optical spectra of II Zw 136 and I Zw 1 show the same differences (Phillips 1978*b*). The strongest emission "line" in the near-infrared is a broad, asymmetric feature with peak near λ8965 (observed wavelength); it is a blend of broad O I λ8446 and Ca II λλ8498, 8542, with Ca II λ8662 visible in its red wing near λ9200 (observed wavelength). It is well shown by

Persson (1988) in his Figure 1. A weaker but definite feature near $\lambda$7502 (observed wavelength) is probably He I $\lambda$7065 (Phillips 1978*b*), or possibly the Fe II $\lambda$7067 unclassified line. A still weaker feature near $\lambda$7770 (observed wavelength), is probably a blend of the two strongest Fe II multiplet (73) lines $\lambda\lambda$7308, 7321. Narrow [S III] $\lambda$9069 is definitely present near $\lambda$9635 (observed wavelength) broad $\lambda$9212 or H I Pa 9 $\lambda$9229 near $\lambda$9800 (observed wavelength), and narrow [S III] $\lambda$9531 near $\lambda$10125 (observed wavelength), so close to the end of the spectrum its intensity is not measurable. The diagnostic information in this spectrum is also briefly discussed in § V.

### *c) NGC 1320*

The only two emission lines seen in our near-infrared spectrum of this high-ionization Seyfert 2 galaxy with redshift $z = 0.0092$ (De Robertis and Osterbrock 1986) are [S III] $\lambda\lambda$9069, 9531 with relative strengths 1.00:2.95. This object is relatively faint, and the signal-to-noise ratio of the available spectrum is correspondingly rather poor; other fainter emission lines may well be detectable on longer exposures.

### *d) VII Zw 31*

This is not a Seyfert galaxy, but an "ultraluminous far-infrared galaxy" with a very high CO luminosity (Sage and Solomon 1987). Its redshift is $z = 0.0544$. On our spectrum, we see in emission only the red wing of a very strong H$\alpha$, blended [S II] $\lambda\lambda$6716, 6731, and fairly strong narrow [S III] $\lambda\lambda$9069, 9531, with measured intensity ratio 1.00:2.76.

## V. INTERPRETATION

The main use of the near-infrared relative line intensities will be in testing and improving calculated photoionization models of active galactic nuclei. The wider the spectral range surveyed, the more lines of more ions can be measured and the more stringent can be the tests of the models. Naturally, the near-infrared data must be combined with measurements made in the optical region at nearly the same epoch. We intend to do this in the future, but we could not do so at the time the somewhat experimental measurements of this paper were being made. Previous optical measurements are available for many of the objects reported here; we prefer to use the Lick data, which were taken in a fairly homogeneous way. References to the measured data, often giving as well the interstellar reddening coefficient which is necessary to convert the measured relative fluxes to intrinsic relative intensities, are Osterbrock and Koski (1976) for NGC 4151, Osterbrock (1977) for NGC 3227, NGC 3516, I Zw 1, and II Zw 136, Phillips (1978*b*) for I Zw 1 and II Zw 136, Koski (1978) for Mrk 1 and Mrk 3, Osterbrock (1981) for III Zw 77, Cohen (1983) for NGC 3227 and NGC 7469, and Osterbrock and Pogge (1985) for Mrk 1126. The main problem is always linking up the infrared and optical measurements.

In addition, new measurements have been made for this paper from previously obtained spectra of NGC 4051, NGC 6814, Mrk 915, and Mrk 993. All these spectra (except one of Mrk 915) were taken with the Image-Dissector Scanner at a resolution of about 10 Å, as previously described, for instance, by Osterbrock (1977) or Cohen (1983). A journal of observations for these spectra is given in Table 6, and the relative line-intensity measurements are given in Table 7.

Another large number of measurements of near-infrared spectra of Seyfert galaxies, many of them southern objects, has been published by Morris and Ward (1988). They did measure the lines in the optical and infrared parts of the spectrum at the same epochs. Some idea of the accuracy of the observed relative line intensities may be obtained by comparison of the theoretical and measured intensities of two forbidden lines from the same upper level. These ratios are independent of excitation conditions or mechanisms and depend only upon ratios of transition probabilities, which are relatively well determined. For [S III] $\lambda9531/\lambda9069$, the calculated ratio is 2.5 (Mendoza 1983), our measured average value is $2.7 \pm 0.7$, and their averaged measured value is $2.4 \pm 0.7$. For [Ar III] $\lambda7136/\lambda7751$, the calculated ratio is 4.1, our measured average is $4.2 \pm 1.0$, and Morris and Ward's measured average is $2.8 \pm 1.1$. (In each case, the standard deviation of a single measured ratio from the mean is given, not an estimated of the error of the mean.)

One interesting comparison is the line ratio [Ar III] $\lambda7136/$[S III] $\lambda9069$, which is relatively independent of ionization level. For our AGN sample as well as for that of Morris and Ward (1988), the average value of this ratio is $0.26 \pm 0.11$, while for six planetary nebulae with published near-infrared spectra (Kaler *et al.* 1976; Aller and Czyzak 1983), the same ratio is $0.55 \pm 0.32$. Thus, though the ranges overlap, there is a significant difference in mean values. Whether this is an abundance difference or a result dependent on the shape of the photoionizing spectra can only be settled by computed models.

[S III], with ground electron configuration $3s^2 3p^2$, is analogous to [O III] of the next lower row in the periodic table, with ground configuration $2s^2 2p^2$. This is one of the main reasons the [S III] $\lambda\lambda$9069, 9531 emission lines are, like their analogs [O III] $\lambda\lambda$4959, 5007, almost ubiquitous in Seyfert galaxies and

TABLE 6

JOURNAL OF OBSERVATIONS: OPTICAL SPECTRA

| Object | UT Date | $\lambda_c$ (Å) | Exposure (Minutes) |
|---|---|---|---|
| NGC 4051 .......... | 1977 Jan 18 | 7701 | 24 |
| | 1977 Mar 26 | 4650 | 16 |
| | 1977 Mar 26 | 5960 | 16 |
| NGC 6814 .......... | 1976 Sep 1 | 4790 | 16 |
| | 1976 Sep 1 | 6790 | 16 |
| Mrk 915 ............ | 1981 Aug 22 | 4650 | 32 |
| | 1981 Aug 22 | 5900 | 32 |
| | 1984 Oct 21* | 6925 | 30 |
| Mrk 993 ............ | 1983 Aug 15 | 4670 | 32 |
| | 1983 Aug 15 | 5795 | 32 |

* CCD spectrograph, resolution 15 Å.

TABLE 7

SEYFERT GALAXIES: OPTICAL RELATIVE LINE INTENSITIES

| Ion | $\lambda_0$ | NGC 4051 | $I(\lambda)/I(H\beta)$ Mrk 915 | Mrk 993 |
|---|---|---|---|---|
| H$\beta$(b) .................. | 4861 | 0.32: | 0.64 } | 1.00 |
| H$\beta$(n) .................. | 4861 | 0.68: | 0.36 } | |
| [O III] .................. | 5007 | 0.86 | 4.2 | 5.5 |
| [O I] .................. | 6300 | 0.068 | 0.21 | 1.3 |
| [S III] .................. | 6312 | 0.008: | 0.028 | ... |
| [Fe X] .................. | 6375 | 0.054 | 0.02: | ... |
| H$\alpha$($b + n$) .............. | 6563 | 2.4 | 7.4 | 5.5 |
| [N II] .................. | 6583 | 0.33: | 0.63 | 11.2 |
| [S II] .................. | 6724 | 0.17 | 0.65 | 4.7 |
| [Ar III] .................. | 7136 | 0.026 | 0.13 | ... |
| [O II] .................. | 7324 | 0.028 | 0.087 | ... |

nebulae. It is possible to determine a mean temperature in the $S^{++}$ zone from the ratio ($\lambda$9069 + $\lambda$9531)/$\lambda$6312, which is analogous to [O III] ($\lambda$4959 + $\lambda$5007)/$\lambda$4363. The determination depends weakly on electron density for $N_e \lesssim 10^5$ cm$^{-3}$ and more critically upon it at higher densities. The main problems with measuring the [S III] ratio are de-blending [S III] $\lambda$6312 from the usually considerably stronger [O I] $\lambda$6300, and correcting for reddening between $\lambda$9531 and $\lambda$6312 to find the intrinsic ratio. From the objects with optical measurements either previously published or listed in Table 7, we were able to find five with measured [S III] $\lambda$6312 fluxes whose optical and near-infrared measurements could be linked up. This was done with the fluxes of [Ar III] $\lambda$7136 and [O II] $\lambda$7324 measured in both regions. They are listed in Table 8, in which the second column gives the measured flux ratio. The reddening constant $c$ (as defined, for instance, in Osterbrock 1989) for NGC 4151 was estimated from the ratio of the narrow components of H$\alpha$/H$\beta$, assuming the intrinsic ratio 3.10 applicable to AGNs, which includes a contribution from collisional excitation (Gaskell 1983; Gaskell and Ferland 1984) while for Mrk 3, it was taken from Koski (1978), corrected to the same intrinsic ratio. For NGC 4051, $c$ (as determined for the NLR) was taken from Dahari and De Robertis (1988); for III Zw 77, an estimated value based on Osterbrock (1981) and Ferland and Osterbrock (1987) was used, and for the NLR of Mrk 915, a very rough estimate, the mean of the other four objects in the table rounded off to one significant figure, was used. These reddening constants are listed in Table 8. The average interstellar extinction curve from Table 7.2 of Osterbrock (1989) was then used to correct the [S III] ratios for reddening. It is, of course, based on data obtained from stars in our Galaxy not too far from the Sun, and to apply it to the dust mixed with near-ionized gas in AGNs is a great extrapolation. The resulting intrinsic [S III] ratios and the mean temperatures derived from them, for assumed electron densities $N_e \to 0$ and $N_e = 10^5$ cm$^{-3}$, are listed in the last two columns of Table 8. These calculations were made using the program of De Robertis, Dufour, and Hunt (1987), which incorporates all the current best data on collision strengths and transition probabilities.

The [S III] temperatures thus determined are fairly well in line with those expected, except that the value for III Zw 77 is rather high. This unusual, high-ionization Seyfert 1 galaxy also has extremely anomalous [O III] ratios, which may indicate some shock heating as well as photoionization heating in this object (Ferland and Osterbrock 1987). Under photoionization conditions, the [S III] and [O III] emitting regions have almost no overlap, because the ionization potential of $S^{++}$, 34.8 eV, is almost the same as that of $O^+$, 35.1 eV. Therefore the mean [S III] and [O III] temperatures are not expected to be the same. In general, from our data, the [S III] values are somewhat higher, but not much higher, than the [O III] temperatures (Koski 1978; Cohen 1983).

One of the most interesting applications of the near-infrared spectral region, at least in principle, would be to determine the interstellar extinction from the ratio of the [S II] $\lambda\lambda$4069, 4076 and $\lambda\lambda$10287–10370 emission lines, which arise from the same upper $^2P$ term. This method was suggested by Miller (1968) and applied by Wampler (1968, 1971) to several Seyfert galaxies, including NGC 4151. It has recently been tested and found to give reasonable results for NGC 1976 by Greve *et al.* (1989). We have attempted to use our measurements of NGC 4151 in this same way. Using the two reasonably strong features in common between Table 3 and the optical measurements of Osterbrock and Koski (1976), $\lambda$7136 and $\lambda$7324, to connect the near-infrared and optical spectra, the measured values are $I(\lambda10287)/I(\text{H}\beta\text{n}) = 0.046$ and $I(\lambda10320)/I(\text{H}\beta\text{n}) = 0.066$. The optically measured ratio from the same paper is $I(\lambda4072)/I(\text{H}\beta\text{n}) = 0.38$, giving $I(\lambda10287 + \lambda10320)/I(\lambda4072) = 0.29$. Using the calculated ratios of the other two [S II] near-infrared lines to the two observed, the "measured" result is $I(\lambda10287\text{–}10370)/I(\lambda4072) = 0.48$. This is *bluer* than the calculated ratio $I(\lambda10287\text{–}19370)/I(\lambda4072) = 0.67$, a quite unphysical result. It could only occur if the dust absorption in the AGN were greater in the near-infrared than in the violet spectral region. All the [S II] calculated ratios are essentially independent of density and temperature (to $\pm$0.01 in the final result) over the range $10^2$ cm$^{-3} \lesssim N_e \leq 10^6$ cm$^{-3}$ and $10^4$ K $\leq T \leq 2 \times 10^4$ K. One possible error is in the measured strength of the [S II] $\lambda\lambda$4069, 4076 doublet; Boksenberg *et al.* (1975) measured $I(\lambda4072)/I(\text{H}\beta\text{n}) = 0.28$ which, combined with our near-infrared value, gives $I(\lambda10287\text{–}10370)/I(\lambda4072) = 0.65$. This value would correspond to essentially zero reddening, within the errors of observation. Wampler (1968) measured $I(\lambda10287\text{–}10370)/I(\lambda4072) = 1.3$, a much different value from ours, and then modified this later to 1.2 or smaller, with some uncertainty. The discrepancies among the different results are large, and the result is important. The sensitivity is low in the $\lambda$10300 region, and in addition, the removal of the flaw at $\lambda$10381 may have affected our measurement of the [S II] lines. Clearly, more observational effort is appropriate.

However, it must also be pointed out that although Wampler (1968, 1971), Boksenberg *et al.* (1975), and Osterbrock and Koski (1976) all attributed the feature near $\lambda$4072 to [S II], Osterbrock (1981) later identified an emission line near $\lambda$4071 in III Zw 77 with [Fe V]. The profile of the line in that galaxy shows practically no contribution from the [S II] doublet. NGC 4151 is, like III Zw 77, a high-ionization object. Though the profile of the feature in NGC 4151 (on a high-resolution spectrum obtained in 1980) clearly shows it is dominated by the [S II] blend, a not inconsiderable contribution may also come from the [Fe V] line. This would tend to make

TABLE 8

[S III] ($\lambda$9069 + $\lambda$9531)/$\lambda$6312 RATIOS AND CALCULATED MEAN TEMPERATURES

| Object | Measured Ratio | Reddening Constant ($c$) | Intrinsic Ratio | $T$ (K) ($N_e \to 0$ cm$^{-3}$) | $T$ (K) ($N_e = 10^5$ cm$^{-3}$) |
|---|---|---|---|---|---|
| NGC 4051 ............ | 62.0 | 0.35 | 43.9 | 11,900 | 10,100 |
| NGC 4151 ............ | 22.3 | 0.19 | 18.4 | 21,400 | 16,200 |
| Mrk 3 .................. | 36.0 | 0.63 | 19.3 | 20,300 | 15,800 |
| Mrk 915 ............... | 52.8 | [0.4] | 35.6 | 13,300 | 11,000 |
| III Zw 77 .............. | 21.0 | 0.30 | 15.6 | 26,100 | 18,600 |

the observed ratio too blue and not directly interpretable in terms of reddening alone.

More qualitative information on the physical conditions in the NLR is available for I Zw 1 and II Zw 136. These galaxies, particularly the former, show only extremely weak forbidden lines in their spectra. From the near absence of [S III], with critical density $N_c \approx 6 \times 10^5$ cm$^{-3}$, and the great weakness of [O III], with $N_c \approx 7 \times 10^5$ cm$^{-3}$, in the spectrum of I Zw 1, the mean electron density in the narrow-line region of this object is probably $N_e \gtrsim 10^7$ cm$^{-3}$. The [Ca II] $\lambda\lambda$7291, 7324 lines are well resolved and definitely narrower than the permitted H I, Fe II, and Ca II lines. The critical density for these lines is $N_c \approx 10^7$ cm$^{-3}$ (see Appendix), and their presence in the observed spectrum implies that there is a very low-ionization NLR, probably with mean $N_e \approx 10^7$–$10^8$ cm$^{-3}$. The relative strengths of the two [Ca II] lines depends on the excitation mechanism, which is probably a combination of collisional and resonance-fluorescence in this case (Ferland and Persson 1989). However, the fact that $\lambda$7324 is not much stronger than $\lambda$7291 shows that it contains only a small contribution from [O II] $\lambda$7324. Since the critical density for this blend is $N_c \approx 5 \times 10^6$ cm$^{-3}$, it cannot be strongly collisionally de-excited. Thus, most of the O in the $Ca^+$ zone that emits [Ca II] is probably in the atomic form $O^0$, and the H therefore probably is also in the corresponding form $H^0$.

## VI. GENERAL CONCLUSIONS

Qualitatively, [S III] $\lambda\lambda$9069, 9531 are strong in all Seyfert galaxies except the very dense objects with usually dense or weak NLRs, such as I Zw 1 and II Zw 136. At shorter wavelengths, [Ar III] $\lambda$7136 and [O II] $\lambda$7324 are observed in nearly all Seyfert galaxies also. The strong atmospheric absorption features, together with the strong OH night-sky emission bands, make near-infrared measurements more difficult than in the optical region, but the information from the near-infrared emission lines is needed for a more complete understanding of the nature of these objects. The best additional diagnostic information it provides, the [S III] ($\lambda$9069 + $\lambda$9531)/$\lambda$6312 ratio, is not as useful as the analogous [O III] ratio, due to the blending of $\lambda$6312 and the greater wavelength interval from $\lambda$6312 to $\lambda$9531, placing greater demands on the reddening and the flux calibration. Finally, a puzzling discrepancy exists among the various observational measurements of [S II] $I(\lambda10287$–$\lambda10370)/I(\lambda4072)$ in NGC 4151.

We are grateful to the referee, Simon L. Morris, for several suggestions which improved this paper, one of which was the identification of several lines of multiplet (1) of N I in NGC 1976. We are grateful for partial support of this research by NSF grant AST 86-11457. Development of the Lick Observatory data acquisition and reduction software was partially supported by NSF grant AST 86-11457. S. V. would like to thank the Natural Sciences and Engineering Research Council of Canada and the FCAR program of the Province of Québec for their financial support.

## APPENDIX

## CRITICAL ELECTRON DENSITY FOR [Ca II]

The critical density for collisional de-excitation of an upper level with one downward radiative transition is well known to be

$$N_c = \frac{A_{j1}}{q_{j1}} ,$$

where $A_0$ is the radiative transition probability and

$$q_{j1} = \frac{8.627 \times 10^{-6}}{\sqrt{T}} \frac{\langle \Omega_{j1}(T) \rangle}{g_j} ,$$

is the collisional de-excitation probability per unit electron density, with $\langle \Omega_{j1}(T) \rangle$ the mean collision strength for the corresponding transition. For [Ca II], $j = 3\,^2D_{3/2}$ and $3\,^2D_{5/2}$, $A_{j1} = 0.92$ s$^{-1}$ and 0.95 s$^{-1}$, respectively (Zeippen 1989), with a mean value of 0.94 s$^{-1}$ to sufficient accuracy. The collision strength $\Omega$ ($3\,^2S$, $4\,^2D$) has been calculated as a function of energy by Saraph (1970). Numerical values for $N_c$ are listed in Table 9, and it can be seen that over the temperature range of interest $N_c \approx 10^7$ cm$^{-3}$ is a good approximate value.

TABLE 9

CRITICAL DENSITY FOR COLLISIONAL DE-EXCITATION OF Ca II

| $T$ (K) | $\langle \Omega(4\,^2S, 3\,^2D) \rangle$ | $N_c$ (cm$^{-3}$) |
|---|---|---|
| 5000 | 13.4 | $5.7 \times 10^6$ |
| 10000 | 11.7 | $9.3 \times 10^6$ |
| 15000 | 10.5 | $1.3 \times 10^7$ |

## REFERENCES


Aller, L. H., and Czyzak, S. J. 1983, *Ap. J. Suppl.*, **51**, 211.
Andrillat, Y., and Collin-Souffrin, S. 1975, *Astr. Ap.*, **43**, 419.
Barnett, E. W., and McKeith, C. D. 1988, *M.N.R.A.S.*, **234**, 241.
Boksenberg, A., Shortridge, K., Allen, D. A., Fosbury, R. A. E., Penston, M. V., and Savage, A. 1975, *M.N.R.A.S.*, **173**, 381.
Bowen, I. S. 1960, *Ap. J.*, **132**, 1.
Cohen, R. D. 1983, *Ap. J.*, **273**, 489.
Dahari, O., and De Robertis, M. M. 1988, *Ap. J. Suppl.*, **67**, 249.
Dennefeld, M. 1982, *Astr. Ap.*, **112**, 215.
———. 1986, *Astr. Ap.*, **157**, 267.
Dennefeld, M., and Pequignot, D. 1983, *Astr. Ap.*, **127**, 42.
De Robertis, M. M., Dufour, R. J., and Hunt, R. W. 1987, *J.R.A.S. Canada*, **81**, 195.
De Robertis, M. M., and Osterbrock, D. E. 1986, *Ap. J.*, **301**, 327.
Ferland, G. J., and Osterbrock, D. E. 1987, *Ap. J.*, **318**, 145.
Ferland, G. J., and Persson, S. E. 1989, *Ap. J.*, **347**, 656.
Garstang, R. H. 1962, *M.N.R.A.S.*, **124**, 321.
Gaskell, C. M. 1983, *Ap. Letters*, **24**, 43.
Gaskell, C. M., and Ferland, G. J. 1984, *Pub. A.S.P.*, **96**, 393.
Grandi, S. A. 1975*a*, *Ap. J.*, **196**, 465.
———. 1975*b*, *Ap. J. (Letters)*, **199**, L43.
———. 1978, *Ap. J.*, **221**, 501.
Greve, A., McKeith, C. D., Barnett, E. W., and Götz, M. 1989, *Astr. Ap.*, **215**, 113.
Henry, R. B. C. 1987, *Ap. J.*, **322**, 399.
Henry, R. B. C., and Fesen, R. A. 1988, *Ap. J.*, **329**, 693.
Kaler, J. B. 1976, *Ap. J. Suppl.*, **31**, 517.
Kaler, J. B., Aller, L. H., Czyzak, S. J., and Epps, H. W. 1976, *Ap. J. Suppl.*, **31**, 163.
Korista, K. T., and Ferland, G. J. 1989, *Ap. J.*, **343**, 678.
Koski, A. T. 1978, *Ap. J.*, **223**, 56.
Lauer, T. R., Miller, J. S., Osborne, C. S., Robinson, L. B., and Stover, R. J. 1984, *Proc. Soc. Photo-Opt. Instrum. Eng.*, **445**, 132.
Mazzarella, J. M., and Balzano, V. A. 1986, *Ap. J. Suppl.*, **62**, 751.
Mendoza, C. 1983, in *IAU Symposium 103, Planetary Nebulae*, ed. D. R. Flower (Dordrecht: Reidel), p. 143.
Miller, J. S. 1968, *Ap. J. (Letters)*, **154**, L87.
Moore, C. E. 1945, *A Multiplet Table of Astrophysical Interest, Revised Edition* (Contributions from the Princeton University Observatory, No. 20).
Morgan, L. A. 1971, *M.N.R.A.S.*, **153**, 393.
Morris, S. L., and Ward, M. J. 1988, *M.N.R.A.S.*, **230**, 639.
———. 1989, *Ap. J.*, **340**, 713.
Netzer, H., and Wills, B. J. 1983, *Ap. J.*, **275**, 445.
Nussbaumer, H., and Storey, P. J. 1980, *Astr. Ap.*, **89**, 308.
———. 1982, *Astr. Ap.*, **110**, 295.
———. 1988, *Astr. Ap.*, **193**, 327.
Oke, J. B., and Gunn, J. E. 1983, *Ap. J.*, **266**, 713.
Osterbrock, D. E. 1977, *Ap. J.*, **215**, 733.
———. 1981, *Ap. J.*, **246**, 696.
———. 1989, *Astrophysics of Gaseous Nebulae and Active Galactic Nuclei* (Mill Valley: University Science Books).
Osterbrock, D. E., and Koski, A. T. 1976, *M.N.R.A.S.*, **176**, 61P.
Osterbrock, D. E., and Pogge, R. W. 1985, *Ap. J.*, **297**, 166.
Osterbrock, D. E., and Shaw, R. A. 1988, *Ap. J.*, **327**, 89.
Osterbrock, D. E., Veilleux, S., and Tran, H. D. 1990, in preparation.
Persson, S. E. 1988, *Ap. J.*, **330**, 751.
Persson, S. E., and McGregor, P. J. 1985, *Ap. J.*, **290**, 125.
Phillips, M. M. 1976, *Ap. J.*, **208**, 37.
———. 1978*a*, *Ap. J.*, **226**, 736.
———. 1978*b*, *Ap. J. Suppl.*, **38**, 187.
Sage, L. J., and Solomon, P. M. 1987, *Ap. J. (Letters)*, **321**, L103.
Saraph, H. E. 1970, *J. Phys. B*, **3**, 952.
Sargent, W. L. W. 1968, *Ap. J. (Letters)*, **152**, L31.
Svensson, L. A., Ekberg, J. O., and Edlen, B. 1974, *Solar Phys.*, **34**, 173.
Wampler, E. J. 1968, *Ap. J. (Letters)*, **154**, L53.
———. 1971, *Ap. J.*, **164**, 1.
Zeippen, C. J. 1989, *Astr. Ap.*, in press.



DONALD E. OSTERBROCK: Lick Observatory, University of California, Santa Cruz, CA 95064

RICHARD A. SHAW: Goddard Space Flight Center, Mail Code 684.9, Greenbelt, MD 20771

SYLVAIN VEILLEUX: Institute for Astronomy, University of Hawaii, 2680 Woodlawn Drive, Honolulu, HI 96822